Limnol. Oceanogr., 53(4), 2008, 1252–1265
© 2008 by the American Society of Limnology and Oceanography, Inc.

Temporal and vertical variability in photosynthesis in the North Pacific Subtropical Gyre

Guido Corno,[1] *Ricardo M. Letelier,*[2] *and Mark R. Abbott*
College of Oceanic and Atmospheric Sciences, Oregon State University, 104 COAS Administration Building, Corvallis, Oregon 97331-5503

David M. Karl
School of Ocean and Earth Science and Technology, University of Hawaii, Honolulu, Hawaii 96822

Abstract

In situ fast-repetition-rate fluorometric (FRRF) surveys were conducted in the North Pacific Subtropical Gyre (NPSG) at Station ALOHA (Sta. ALOHA, 22°45′N, 158°00′W), from September 2002 to December 2004, to assess temporal and vertical photosynthetic variability in relation to environmental conditions. The nighttime potential photosynthetic efficiency of the photoautotrophic microbial assemblage (given as the ratio of variable to maximal fluorescence, $F_V : F_M$) was low in the mixed layer and increased with depth. High $F_V : F_M$ values were observed at and below the deep chlorophyll maximum layer (DCML); some values approached the theoretical maximum for prokaryotes grown under nutrient-replete conditions in the laboratory (0.60). In contrast, the absorption cross section of photosystem II (σ_{PSII}) was high at the surface and decreased with depth; minima (1,000 Å^2 quanta^{-1}) occurred around the DCML. These vertical patterns suggest photosynthetic stress conditions in surface photoautotrophic populations. No significant seasonal cycles were found for $F_V : F_M$, but surface σ_{PSII} values peaked in winter and decreased during summer, suggesting that seasonal variations in light availability may influence the observed σ_{PSII} variability. A significant correlation was found among surface $F_V : F_M$, σ_{PSII}, and the distance from the mixed-layer depth (MLD) to the top of the nutricline. Neither nutrient nor light variations were significantly related to $F_V : F_M$ and σ_{PSII} in the DCML. Within this layer, $F_V : F_M$ variability was positively and negatively related to concentrations of chlorophyll *b* and zeaxanthin, respectively. Our results suggest that, at Sta. ALOHA, surface photosynthesis takes place under chronic nutrient limitation, while higher photosynthetic efficiency in the lower euphotic zone appears to be sensitive to community-structure changes.

In the ocean, variations in photosynthetic rates across different spatial and temporal scales can significantly influence ecosystem dynamics, including fishery yields and carbon sequestration (DiTullio and Laws 1991; Falkowski et al. 1998; Letelier et al. 2000). However, in oligotrophic regions of the ocean, these variations have been considered small due to chronic nutrient limitation (Berger 1989). This oligotrophic condition controls organic matter (dissolved and particulate) production and export (Karl 1999) and influences physiological and ecological adaptations of photoautotrophic organisms (Karl et al. 2001).

In the North Pacific Subtropical Gyre (NPSG), low assimilation numbers (i.e., light-saturated rates of gross carbon fixation normalized to total chlorophyll *a*) have been interpreted as evidence of nutrient limitation of photosynthetic processes (Karl et al. 1996; Letelier et al. 1996). However, large (<200 and >900 mg C m^{-2} d^{-1}), aperiodic variations from long-term mean (450 mg C m^{-2} d^{-1}) production rates have also been observed in this region (DiTullio and Laws 1991; Karl et al. 2001). These variations span different temporal scales (days to months) and are related to a variety of independent physical forcing events (e.g., variations in isolume depths, internal waves, mesoscale eddies, planetary Rossby waves; Letelier et al. 2000; Karl et al. 2001; Sakamoto et al. 2004). Temporal fluctuations in physical environment can alter the quantum yield of photosynthesis (herein identified as the in situ quantum efficiency of carbon fixation, ΦC, with units of mol C mol quanta^{-1}) of the photoautotrophic assemblage.

A comprehensive understanding of the environmental factors (abiotic and biotic) that control ΦC variability in the NPSG over high-frequency temporal (hours to days) and small spatial (meters) scales has not yet been achieved due to methodological limitations. The ^{14}C radiotracer method (Steeman-Nielsen 1951), which has been widely

[1] Present address: United Nations High Commissioner for Refugees (UNHCR), P.O. Box 1076, Addis Ababa, Ethiopia.

[2] Corresponding author (letelier@coas.oregonstate.edu). Also at: Departamento de Ecologia, Center for Advanced Studies in Ecology & Biodiversity (CASEB), Pontificia Universidad Católica de Chile, Casilla 114-D, Santiago, Chile.

Acknowledgments

The authors thank the captains and crews of the many research vessels that have supported the HOT program since 1988. We also thank all HOT personnel for expert field and laboratory assistance, especially Lance Fujieki for his assistance in overseeing the deployment of the optical instruments, Roger Lukas for leading the HOT Physical Oceanography team, and Amanda Ashe for providing logistical support. Mike Behrenfeld, David J. Suggett, Samuel Laney, and two anonymous reviewers contributed valuable comments to the original manuscript. The present research was supported by National Science Foundation (NSF) grants OCE03-26419 (awarded to R.M.L.) and OCE03-26616 (awarded to D.M.K.) and by a grant from the Gordon and Betty Moore Foundation (awarded to D.M.K.).

used to derive photosynthetic activity in the NPSG (Platt 1984; Karl et al. 1998), has limited temporal resolution due to the requirement for in situ incubation and even more limited spatial resolution because only a few discrete depths are typically analyzed in a given oceanic profile (Peterson 1980). The same restrictions apply to the light–dark oxygen method (Williams et al. 2004) and the $H_2{}^{18}O$ technique for estimation of gross primary production (Grande et al. 1989; Kaiser et al. 2006). In contrast, the triple-oxygen technique is an instantaneous measurement that does not require an incubation step (Juranek and Quay 2005); however, it has a 2–3 week integration timescale, which limits its use in the study of high-frequency events. All these limitations affect the precision and accuracy in assessing water-column integrated photosynthetic activity when interpolating between discrete temporal and vertical measurements. Furthermore, they can significantly affect our understanding of the variability in the metabolic balance of the system, generating a bias against the sampling of the microbial community during mesoscale perturbations, such as the passage of eddies or summer bloom events in the NPSG (Karl et al. 2003).

Fast-repetition-rate fluorometry (FRRF) represents an alternative high-resolution method to characterize both vertical and temporal scales of variability of photosynthetic processes (Kolber et al. 1998). By assessing the photosynthetic efficiency of photosystem II (PSII) through rapid, in situ, repetitive measurements of the fluorescence yield after reducing the primary acceptor quinone (and thus decreasing the probability that the reaction center of PSII [RCII] is photochemically active), FRRF can resolve small vertical (meters) and temporal (seconds) scales, compared to tens of meters and hours/weeks for the methods based on isotopic tracers. In addition, other photosynthetic parameters, such as the functional cross section of PSII (σ_{PSII}), the minimum turnover time of the photosynthetic unit (τ), primary production versus irradiance (P vs. E) curves, electron transport rates (ETR), and gross oxygen evolution rates (GOE), can also be derived using FRRF measurements. The possible bias associated with the inclusion, isolation, trace-metal toxicity, and light shock during ^{14}C and $H_2{}^{18}O$ incubations is also reduced in discrete FRRF sampling or eliminated altogether during in situ FRRF measurements. However, the FRRF method has technical limitations that should be taken into account when interpreting the data. The major technical limitations include the poor sensitivity at low chlorophyll *a* (Chl *a*) concentrations (decrease in the signal-to-noise ratio, which makes it difficult to interpret the fluorescence signal), lack of spectral resolution (flash energy centered at 470 nm, which therefore concentrates mainly on Chl *a* activity), and the measurement restrictions to PSII and not PSI activity (restricting the photoautotrophic characterization to only PSII activity). Nevertheless, a comparison between primary productivity (PP) estimates from FRRF and ^{14}C at Sta. ALOHA has highlighted as in FRRF's potential to determine PP variations in this environment (Corno et al. 2006). Furthermore, this analysis reveals that σ_{PSII} variability can play a significant role in the observed variability in PP at Sta. ALOHA.

Previous attempts to model PP at Sta. ALOHA have highlighted the need to describe the variability of ΦC across different temporal and vertical scales in order to improve the accuracy of the model estimates (Ondrusek et al. 2001). In the present study, time-series FRRF measurements (August 2002–December 2004) are presented and discussed in order to characterize the photosynthetic efficiency and variability across vertical scales not achievable by the ^{14}C and the $H_2{}^{18}O$ techniques. These observations are used to determine the environmental factors that control the photosynthetic efficiency variations at Sta. ALOHA. In particular, the potential roles of chronic nutrient limitation and community structure in determining photosynthetic efficiency are explored.

Methods

Field sampling—Quasi-monthly (between 3 and 5 weeks), in situ nighttime (between midnight and 03:00 h local time) FRRF measurements were obtained at Sta. ALOHA between September 2002 and December 2004 as part of the ongoing Hawaii Ocean Time-Series (HOT) bio-optical component. A full description of the sampling procedure can be found in Corno et al. (2006). Briefly, a FASTTrackA (Chelsea Instruments S/N 182047) FRR fluorometer with dual light and dark chambers was used to measure active fluorescence. The package was lowered at a constant speed of 10 m min^{-1} to a final depth of ~250 m. This speed was empirically determined to: (1) best resolve the fluorescence response of small-scale (~0.5 m) variations in photoautotrophic assemblages, (2) allow enough time for the instrument to switch gains without losing significant vertical resolution, and (3) obtain statistically significant fluorescence saturation curves.

The FRRF protocol consisted of a saturation phase, where 100 excitation flashlets were delivered within 280 μs, and a relaxation phase, where 20 excitation flashlets were delivered within 50 μs. Measurements of minimal and maximal fluorescence in dark-adapted state (F_O and F_M, respectively), and a value termed the variable fluorescence (F_V), defined as the quantity $[F_M - F_O]$, were obtained. The maximum change in the quantum yield of fluorescence (i.e., the efficiency of photosystem II [PSII], indicated by $F_V : F_M = [F_M - F_O] : F_M$), and the effective absorption cross section for PSII, σ_{PSII}, were also derived. In order to obtain statistically significant fluorescence parameters in these low–Chl *a* waters, the quality of the fitted saturation curves to the physiological model of Kolber et al. (1998) was analyzed for different instrument gains. The fluorescence saturation curves were statistically significant (p value < 0.05, $n = 4{,}000$) from the surface to ~200 m. Below 200 m, the fluorescence transients could not be resolved from the instrument noise. The best fit to the model occurred at gain 16 and gain 64 (characteristics of the depth interval 60–160 m), while fluorescence transients at gain 256 (typical at surface to 60 m, and below 160 m) displayed a statistically significant fit but with higher variance (10–15% variance from the physiological model of Kolber et al. 1998; Fig. 1A). In order to assess the data quality for gain 256, fluorescence transients were analyzed

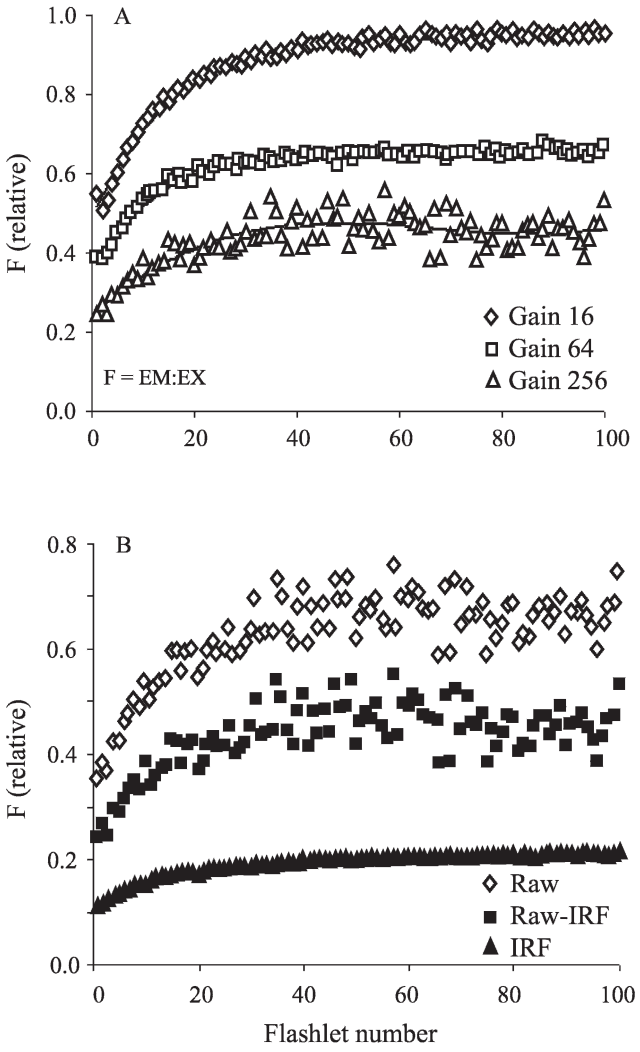


Fig. 1. (A) Variations in the fluorescence yield, F (i.e., obtained by the ratio of emission to excitation flashlets, EM : EX), induced by the saturation FRRF protocol used at Sta. ALOHA for different instrument gain (data shown are from different samples). Solid lines for each saturation curve represent the physiological model used to derive fluorescence parameters (Kolber et al. 1998). Saturation curves are from different samples. (B) Representative FRRF transients for gain 256 at Sta. ALOHA for raw and corrected data (i.e., raw data – IRF at gain 256).

in relation to the instrument response function (IRF) at gain 256 (Fig. 1B) using dilute concentrations of rhodamine B, an inert fluorophore (R-6626, Sigma Chemical; Laney 2003). Only samples where raw FRRF data – IRF values were statistically greater than the IRF were considered to be valid fluorescence transients; samples where no significant difference was found were eliminated. A sensitivity analysis was also performed to understand the possible influence of the FRRF gain (and gain switch) on FRRF parameter derivation and the associated temporal and vertical variability. No significant relationship was found when the entire data set and all gains were considered.

As part of the ongoing HOT program, nitrogen (i.e., $[NO_3^- + NO_2^-]$, N + N) and phosphorus (i.e., soluble reactive phosphorus, SRP) concentrations were determined during each cruise by chemiluminescence (Garside 1982) and magnesium-induced coprecipitation (MAGIC; Karl and Tien 1992), respectively. Pigment concentrations were also determined by reverse-phase high-performance liquid chromatography (HPLC) as described by Letelier et al. (1993). These data sets can be obtained from the Hawaii Ocean Time-Series Data Organization & Graphical System (HOT-DOGS) at http://hahana.soest.hawaii.edu/hot/hot-dogs/interface.html. Potential density, salinity, and temperature data for each cruise were also obtained from HOT-DOGS. Time series of the mixed-layer depth (MLD) were calculated from the HOT-CTD (conductivity, temperature, depth) data archive as the depth where an offset of 0.125 in potential density (σ_θ) from the surface occurred (Levitus 1982). The top of the nutricline was calculated following the derivation by Letelier et al. (2004). Briefly, the top of the nutricline was determined by a cubic spline interpolation for near-inertial oscillation depth corrected for N + N and defined as the shallowest depth at which the N + N depth gradient exceeded 2 μmol m^{-4}. The in situ light at depth z was obtained from the daily-integrated surface light value from the ship's LI-COR sensor, and it was calculated using the appropriate extinction coefficient (0.039 and 0.044 for summer and winter, respectively; Letelier et al. 2004).

FRRF blank determination—After analyzing fluorescence traces (from a Sea-Bird 911 fluorometer) to 1,000-m depth from past CTD profiles in the region, a fluorescence minimum was determined to be present between 200 to 300 m. Seawater from this depth interval was then collected and analyzed in the dark for both light and dark FRRF chambers for the different instrument gains. Similar measurements were made for water collected at 1,000 m and for filtered (0.2 μm) seawater collected at 250 m. Seawater between 200- to 300-m depth had the lowest fluorescence signal (t-test, p value < 0.05, $n = 12$). For each cruise, fluorescence transients below 200 m were then used as a correction blank. The difference between the 200–300-m fluorescence and the other two blanks may have been due to different concentrations of dissolved chlorophyll, other compounds that contribute to soluble fluorescence, or scattering. Although the blank correction used here does not take into account potential changes with pressure and temperature (although it does account for possible temporal variations), it represents a practical solution to this critical correction when dealing with low in situ fluorescence signals, as highlighted by Cullen and Davis (2003).

Data processing and statistical analyses—Data were downloaded from the FRR fluorometer and analyzed using the V6 software (provided by Sam Laney), which represents an updated version of V5 (Laney 2003). The raw data were quality controlled (QC) by (1) eliminating fluorescence measurements that did not significantly fit the saturation curves to the physiological model of Kolber et al. (1998), and (2) subtracting the mean of the blank for F_O and F_M. The ratio $F_V : F_M$ was then recalculated using the F_O and F_M values obtained after blank correction.

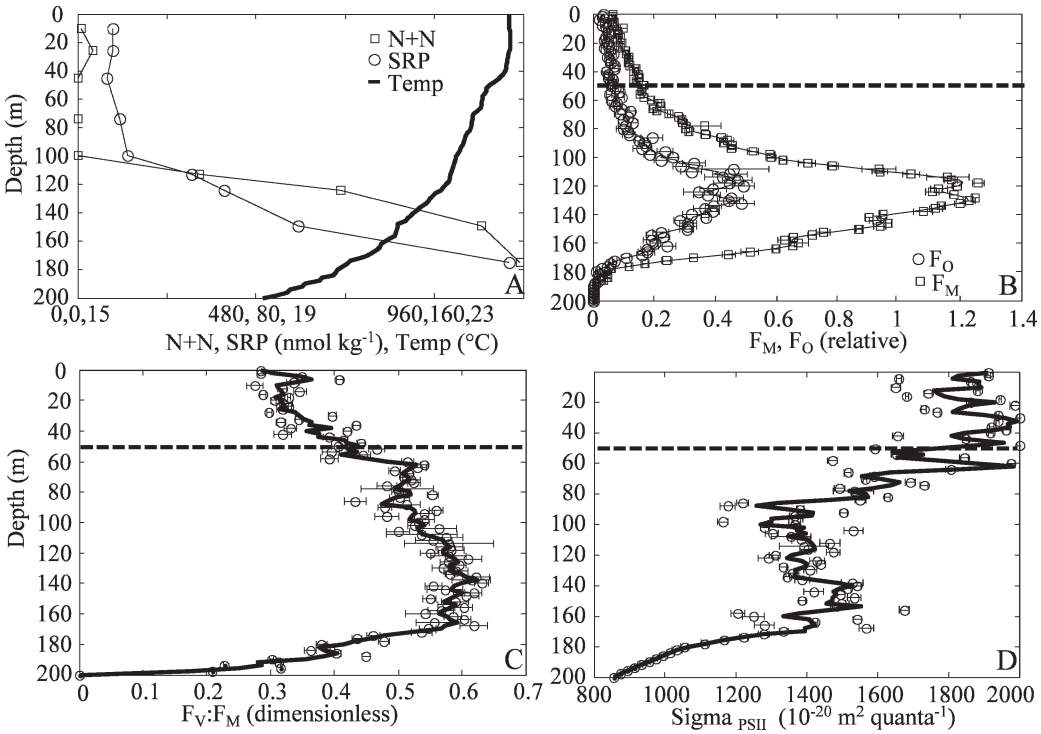


Fig. 2. (A) Vertical profiles of temperature, N + N, SRP, (B) F_O and F_M, (C) $F_V : F_M$, and (D) σ_{PSII} at Sta. ALOHA during HOT-146 (March 2003). In panel A, each tick corresponds to 2°C for temperature (range 15–25°C), 240 nmol kg^{-1} for N + N (range 0–1,200 nmol kg^{-1}), and 40 nmol kg^{-1}for SRP (range 0–200 nmol kg^{-1}). In the fluorescence plots (panels B, C, D), error bars represent ±1 standard error, the solid line represents the 4-point running average, and the horizontal dashed line is the MLD.

Least-squares model II regression analysis and multiple linear regression (MLR, complete and stepwise model) were applied to determine significant correlation coefficients among FRRF parameters (i.e., $F_V : F_M$ and σ_{PSII}) and biological (i.e., HPLC pigments concentrations), chemical (i.e., salinity, N + N and SRP concentrations), and physical (e.g., density, light, and temperature) factors. For each variable, conditions of linearity and normality were evaluated, and, where needed (N + N and SRP), variables were log-transformed to adhere to these statistical conditions. For model II regression, the geometric mean was used to estimate slope and intercept confidence intervals (McArdle 2003). Significant seasonal and vertical differences for each FRRF parameter were tested by *t*-tests and analysis of variance (ANOVA, type I).

Results

General environmental characteristics—Major nutrient concentration profiles (corrected for near-inertial oscillations; Letelier et al. 1996) were low in the upper 100 m during the entire sampling period (Figs. 2, 3). N + N concentrations were <10 nmol kg^{-1}, while SRP values were <50 nmol kg^{-1}. Below 100 m, N + N and SRP values increased sharply to values greater than 800 and 100 nmol kg^{-1}, respectively (Figs. 2, 3). The top of nutricline depth (defined here as in Letelier et al. 2004) was on average around 100 ± 8 m (winter average 90 ± 8 m, $n = 6$; summer average 115 ± 5 m, $n = 5$).

Sea-surface temperature (SST) varied between 26.6°C and 23.3°C (September 2003 and January 2003, respectively); it was higher in summer (25.9 ± 0.1°C, $n = 5$) and decreased in winter (24.0 ± 0.1°C, $n = 6$). The MLD varied between 20 m and 105 m (July 2003 and January 2004, respectively). Mixed-layer depths were shallower during summer months (41 ± 4 m, $n = 5$), while for the rest of the year deeper MLD values were recorded (78 ± 7 m, $n = 6$).

The minimal (F_O) and maximal (F_M) fluorescence displayed similar temporal and vertical patterns. However, greater variability was associated with F_O than F_M. F_M increased with depth and reached maxima between 90 and 120 m (Fig. 4A). This layer of high–Chl *a* fluorescence, previously defined as the deep chlorophyll maximum layer (DCML; Letelier et al. 1996), was deeper in summer (120 ± 2 m, $n = 5$) than in the winter (100 ± 4 m, $n = 6$).

Temporal and vertical variability in photosynthetic efficiency—$F_V : F_M$ was significantly lower at the surface (i.e., 0–10 m) than at the base of the MLD and in the DCML layer (Table 1). In general, $F_V : F_M$ increased with depth, reaching maxima (0.55–0.60) at and below the DCML (Figs. 2, 4B). Below these maxima, $F_V : F_M$ decreased with increasing depth to values indistinguishable from zero, where no active fluorescence was detected. This threshold depth ranged from 160 to 190 m (Fig. 4B).

This clear vertical pattern (i.e., low $F_V : F_M$ at the surface and high $F_V : F_M$ in the DCML) changed during January 2004, when upper-water-column $F_V : F_M$ values increased

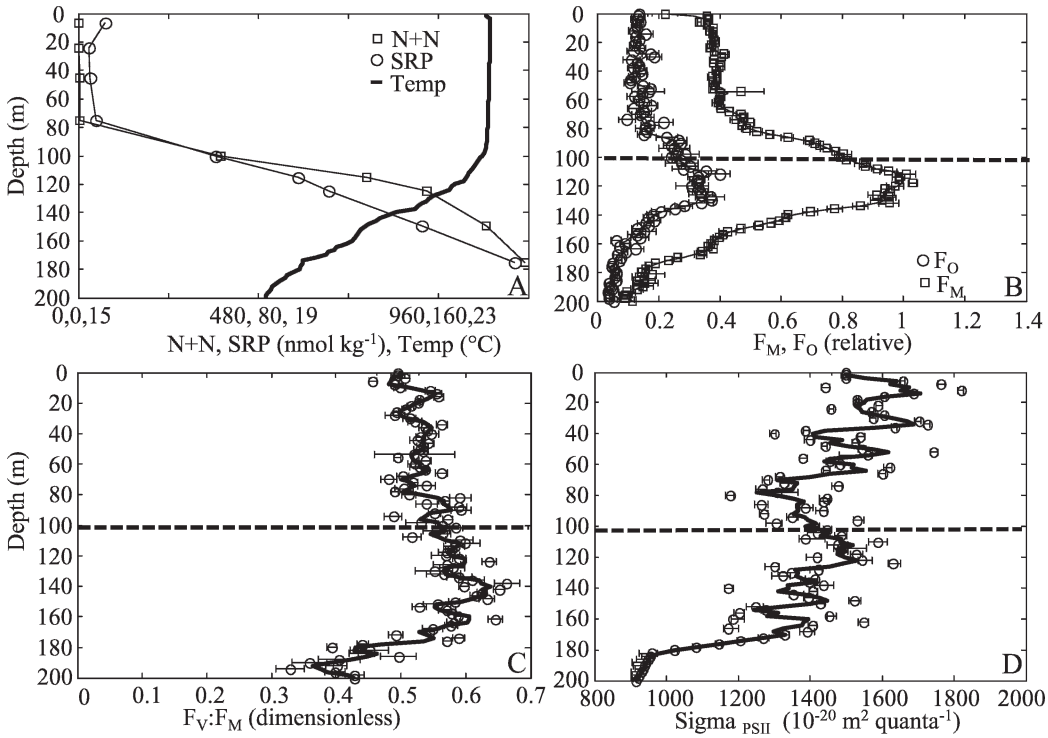


Fig. 3. (A) Vertical profiles of temperature, N + N, SRP, (B) F_O and F_M, (C) $F_V : F_M$, and (D) σ_{PSII} at Sta. ALOHA during HOT-155 (January 2004). In panel A, each tick corresponds to 2°C for temperature (range 15–25°C), 240 nmol kg^{-1} for N + N (range 0–1,200 nmol kg^{-1}), and 40 nmol kg^{-1} for SRP (range 0–200 nmol kg^{-1}). In the fluorescence plots (panels B, C, D), error bars represent ±1 standard error, the solid line represents the 4-point running average, and the horizontal dashed line is the MLD.

to values not significantly different than those at the DCML (*t*-test, $p < 0.05$, $n = 12$) as a result of the mixed layer eroding the top of the nutricline (Figs. 3, 4B). During this period, the $F_V : F_M$ ratio was constant with depth. Conversely, when the MLD was shallower than the nutricline (21 out of 22 times), and was therefore not able to erode the top of the nutricline, a significant increase ($p < 0.05$, $n = 21$) in $F_V : F_M$ was observed from the MLD to layers below the MLD (i.e., 10 m) (Figs. 3, 4B).

In contrast to the well-defined $F_V : F_M$ vertical patterns, no distinct seasonal variations in surface or DCML data were observed (Fig. 5A). However, peaks in $F_V : F_M$ values occurred during winter both at the surface and in the DCML.

Temporal and vertical variability in absorption cross section (σ_{PSII})—Vertical patterns in σ_{PSII} were, to a first approximation, the opposite of those observed for $F_V : F_M$. The values of σ_{PSII} decreased with depth and reached minima (1,000 Å^2 quanta^{-1}) around the DCML (Figs. 2, 4C). Overall, σ_{PSII} was significantly higher at the surface than at the base of the MLD and in the DCML layer (Table 1).

As observed for $F_V : F_M$, upper-water-column σ_{PSII} values were not significantly different (*t*-test, $p < 0.05$, $n = 12$) than those in the DCML during January 2004 (Figs. 3, 4C). During this period, upper-water-column σ_{PSII} values decreased, resulting in a constant trace without trend with depth. Time-series analysis also revealed that during the summer 2003, surface and DCML σ_{PSII} values were significantly different (*t*-test, $p < 0.05$, $n = 12$), even though the MLD was shallower than the top of the nutricline. As for $F_V : F_M$, a significant change ($p < 0.05$, $n = 21$) in σ_{PSII} (lower values) was observed below the MLD, when the MLD was shallower than the nutricline (Figs. 2, 4C).

Unlike the lack of clear temporal $F_V : F_M$ variation, a significant (sinusoidal fit, $p < 0.05$, $n = 22$) seasonal pattern in σ_{PSII} was present at the surface but not at the DCML (Fig. 5B). At the surface, σ_{PSII} maxima occurred during winter, while minima occurred during summer. In the DCML, σ_{PSII} reached a minimum value observed during October 2004, but it varied little for the remaining period.

Relationship between photosynthetic efficiency and chemical–physical factors—Photosynthetic efficiency (all data collected at night) showed correlation with chemical but not physical factors. In particular, no significant relationships were found between FRRF parameters and temperature. On the other hand, considering all the available data sets, $F_V : F_M$ was positively related to N + N but not to SRP; σ_{PSII} was negatively related to both nutrient concentrations (Table 2). However, photosynthetic parameters were not significantly related to nutrient concentrations for surface and DCML samples, respectively.

In order to understand the potential influence of nutrient-diffusion variability on the photosynthetic efficiency in the upper water column, the distance between the MLD and the top of the nutricline was derived as mixed layer depth (m) – nutricline depth (m). Surface and mixed-

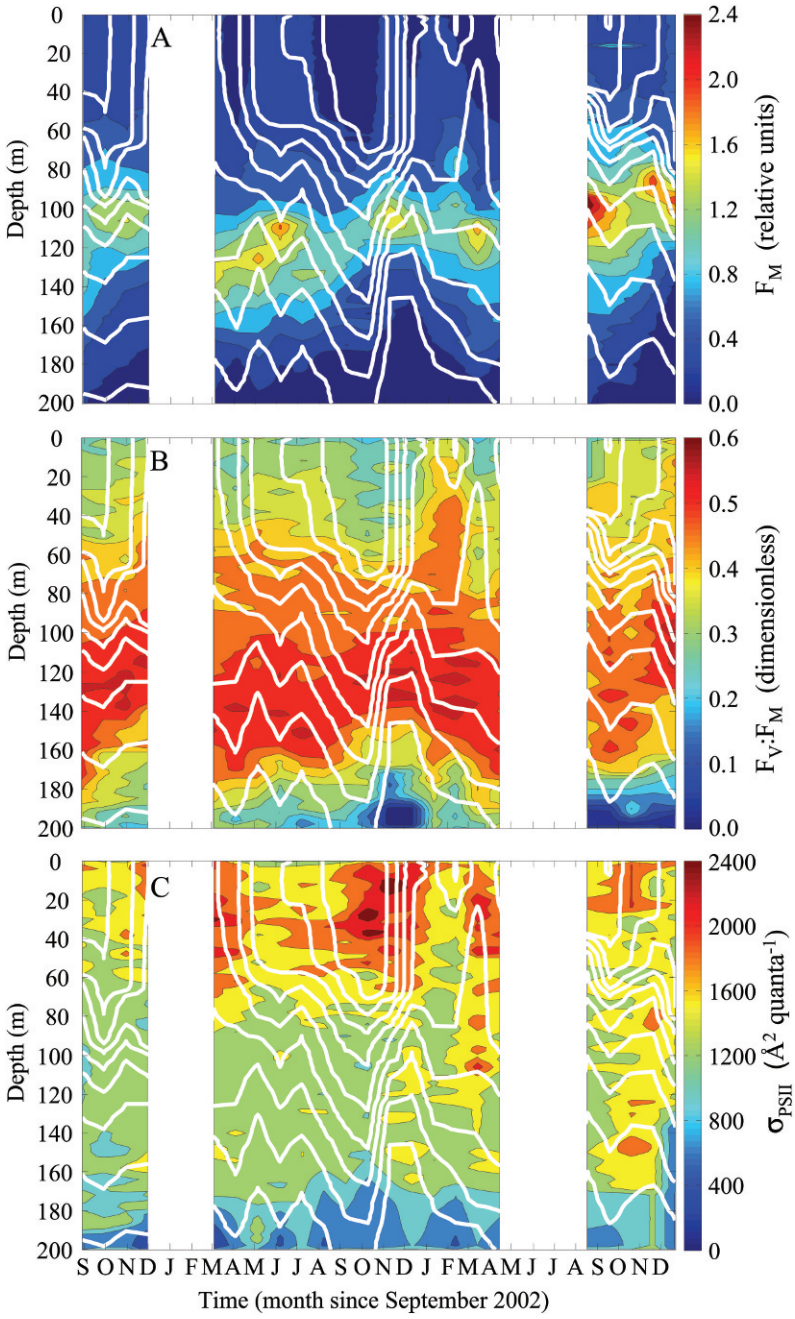


Fig. 4. Vertical and temporal variability in (A) F_M, (B) $F_V:F_M$, and (C) σ_{PSII} at Sta. ALOHA from August 2002 to December 2004. Contours are 0.1 relative units for F_M, 0.05 dimensionless units for $F_V:F_M$, and 250 Å^2 quanta^{-1} for σ_{PSII}. White lines are isopycnal every 0.25 kg m^{-3}.

Table 1. Vertical variations (refer to text for definition of vertical interval) in average $F_V:F_M$ and σ_{PSII} at Sta. ALOHA from August 2002 to December 2004. Values represent the mean ±1 SE for each vertical interval.

	Surface	Base ML (±5 m)	DCML
$F_V:F_M$	0.37±0.01	0.46±0.01	0.55±0.01
σ_{PSII}	1,780±60	1,630±62	1,430±50

layer $F_V:F_M$ values were negatively related to this distance, while a positive relationship was found for σ_{PSII} at the base of MLD (Table 3; Fig. 6). When the MLD was shallower than the top of the nutricline, both $F_V:F_M$ and F_M in the mixed layer were significantly ($p < 0.05$, $n = 1{,}500$; Fig. 7A) lower than at depth. However, when the MLD was deeper than the top of the nutricline, no significant difference between $F_V:F_M$ in the mixed layer and below it was found (Fig. 7B).

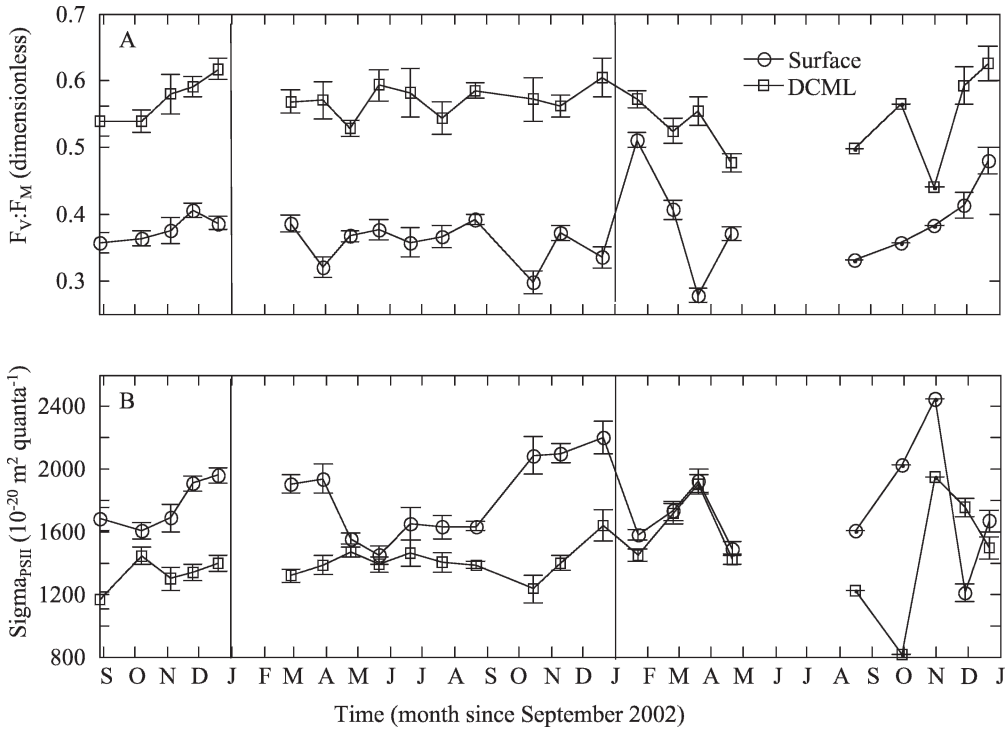


Fig. 5. Temporal variation in (A) $F_V:F_M$ and (B) σ_{PSII} at the surface and the DCML at Sta. ALOHA from August 2002 to December 2004. Vertical lines for each plot indicate the end of year. Error bars represent ±1 standard error.

To further determine the potential role of nutrients versus light in controlling photosynthetic efficiency, variations in DCML depth (corrected for near-inertial oscillations), nutrients, and light were also compared to photosynthetic parameter changes in the DCML. No significant relationships were found between photosynthetic parameters and the physical and chemical factors in this layer.

Photosynthetic efficiency and pigment concentrations—Selected pigments, including chlorophyll *b* (Chl *b*, a biomarker for prochlorophytes), zeaxanthin (Zea, a biomarker for prochlorophytes and cyanobacteria), 19′-hexanoyloxyfucoxanthin (19′-Hex, a biomarker for prymnesiophytes), and fucoxanthin (Fuco, a biomarker for diatoms) (Mackey et al. 1996), were used to assess the role of assemblage composition in the variability of photosynthetic parameters at Sta. ALOHA. The multiple linear regression (MLR) model between pigment concentrations and $F_V:F_M$ was significant for DCML but not for surface samples (Table 4). The MLR model between pigments and σ_{PSII} was not significant for either surface or DCML results. In addition, no significant relationships were found between pigment concentrations and the MLD–nutricline distance and DCML position, respectively. Stepwise MLR indicated that together [Chl *b*] and [Zea] accounted for >95% of $F_V:F_M$ variability in the DCML. In this region, $F_V:F_M$ was positively and negatively related to [Chl *b*] and [Zea], respectively, while no significant relationship was found at the surface (Fig. 8; Table 5). However, the pigment concentrations at the DCML were calculated through extrapolation and are subject to some uncertainty.

Table 2. Statistical parameters for model II linear regression between FRRF parameters and nutrient concentrations at Sta. ALOHA from August 2002 to December 2004. For each significant regression, the slope and confidence interval (CI), the *y*-intercept, and r^2 and *p* values are given.

	$F_V:F_M$		σ_{PSII}	
	log N+N	SRP	log N+N	SRP
Slope	0.034	0.10	−134	−4.60
y-intercept	0.41	0.09	1,852	1,800
CI slope	0.004	0.02	20	0.10
r^2	0.57	0.10	0.20	0.26
p	<0.05	NS	<0.05	<0.05

Table 3. Statistical parameters for model II linear regression between FRRF parameters and the distance from the MLD to the top of the nutricline (refer to text for definition) for different depth intervals at Sta. ALOHA from August 2002 to December 2004. For each significant regression, the slope and confidence interval (CI), the *y*-intercept, and the r^2 and *p* values are given.

	$F_V:F_M$		σ_{PSII}	
	Surface	Base ML (±5 m)	Surface	Base ML (±5 m)
Slope	−0.0024	−0.0029	NS	983
y-intercept	0.44	0.60	NS	22
CI slope	0.007	0.008	NS	250
r^2	0.60	0.74	NS	0.63
P	<0.05	<0.05	NS	<0.05

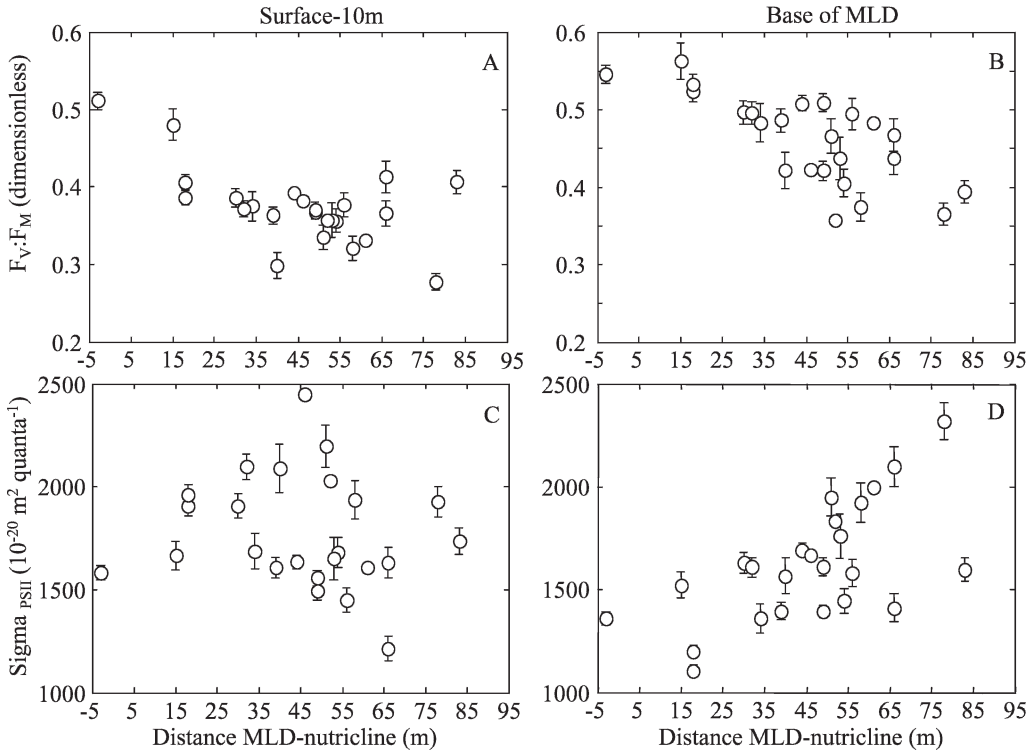


Fig. 6. Relationships among $F_V:F_M$, σ_{PSII}, and the distance from the MLD to the top of the nutricline (as defined in the text) for (A, C) the surface and (B, D) the MLD samples, respectively. Error bars represent ±1 standard error. The statistical parameters for the regression are given in Table 3.

Discussion

At Sta. ALOHA, the photosynthetic efficiency was low in the upper water column, but it increased in the lower euphotic zone. This vertical difference appeared to be the result of two distinct environmental conditions. While a chronic substrate limitation seemed to control photosynthetic processes in surface layers, community-structure changes appeared to contribute to the observed variability in photosynthetic efficiency in the lower euphotic zone. The vertical difference in photosynthetic efficiency and relative controlling factors has added a new perspective to the previously proposed two-layer model for this oligotrophic ocean (Coale and Bruland 1987).

In our study, the variability of $F_V:F_M$ and σ_{PSII} are interconnected through modification of light harvesting and light utilization. $F_V:F_M$ and σ_{PSII} modification can occur through acclimation and inhibition (i.e., at the phenotypic level) but also adaptation (i.e., at the genotypic level). These two processes are separated by the timescale over which environmental variability operates. The data presented here demonstrate that in the vertical scale (a timescale corresponding to the rate of mixing), the availability of nutrients sets constraints on $F_V:F_M$ and σ_{PSII}; thus, the inhibition component is strong. At longer temporal scales (i.e., months), acclimation and adaptation processes affect the variability of $F_V:F_M$ and σ_{PSII}. This study also presents circumstantial evidence that at any given depth, one or both processes may be operating.

Vertical gradient in photosynthetic efficiency and associated environmental forcing—The photosynthetic efficiency, as indicated by $F_V:F_M$, is a function of light, nutrients, temperature, species composition, and the recent history of environmental conditions. At Sta. ALOHA, the overall photosynthetic efficiency appeared to be correlated mainly with the availability of nutrients (in particular, N + N; Table 2). The maxima in $F_V:F_M$ were observed at and below the top of the nutricline, consistent with previous laboratory and field studies for nutrient-replete photoautotrophs (Kolber and Falkowski 1993; Kolber et al. 1998; Suggett et al. 2003). These maxima occurred within a region in the euphotic zone (i.e., DCML) where the vertical diffusive flux of inorganic nutrients is greatest (Dore and Karl 1996). This constant supply of inorganic substrate, mainly N + N, can induce a greater efficiency in PSII activity by increasing the number of functional RCIIs.

The role of nutrients in controlling photosynthetic efficiency was also indicated by the significant relationships between surface photosynthetic parameters and the distance between the base of the MLD and the top of the nutricline (MLD – the top of the nutricline). Even though there is not a clear physical explanation to this relationship, this distance may serve as a proxy for the undetectable flux of nutrients into the euphotic zone. The significant relationship between this distance and surface photosynthetic efficiency can then be interpreted as an indication of nutrient control on surface photosynthetic processes. However, this proxy still requires a theoretical biophysical

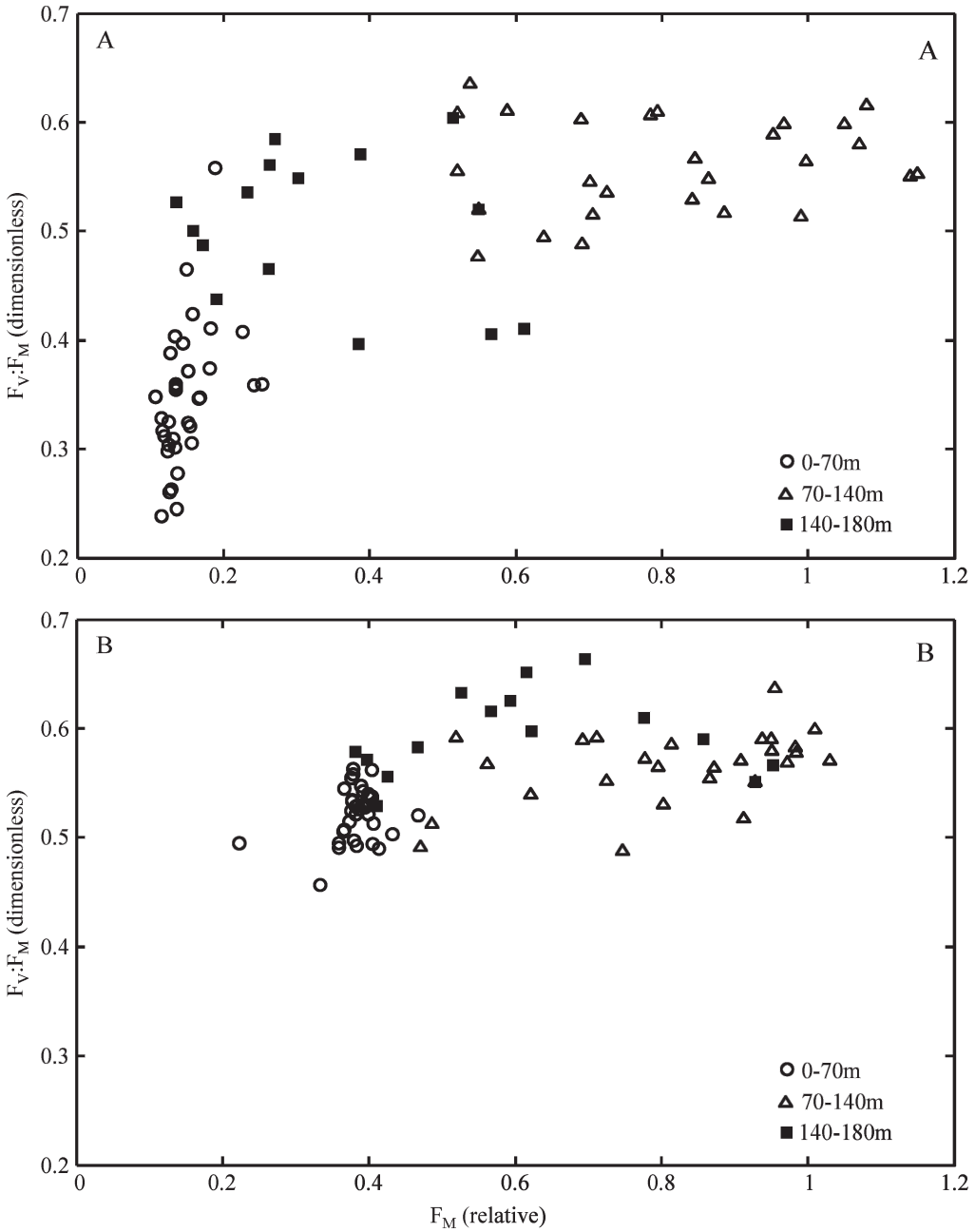


Fig. 7. Relationship between $F_V : F_M$ and F_M at Sta. ALOHA when the MLD was (A) shallower (HOT-146) and (B) deeper (HOT-155) than the top of the nutricline, respectively.

derivation linking this distance to the vertical nutrient diffusive flux, as it assumes a negligible horizontal diffusion and constant entrainment in the MLD. Alternatively, the observed relationship between surface photosynthetic processes and the distance from the MLD to the top of the nutricline could be linked to the activity of vertical migrants (i.e., diatoms containing N_2-fixing endosymbionts and *Trichodesmium* spp.) in relation to stratification dynamics through decoupling of the physical dependence of nutrient delivery in the upper water column (Karl et al. 1992). The role of nutrient availability in controlling surface photosynthetic efficiency is also supported by regression with other environmental parameters. The lack of significant relationships between (1) surface photosynthetic parameters versus surface pigment concentrations and (2) surface pigment concentrations versus the distance from the MLD to the nutricline suggests that variations in community structure are not significantly influencing the observed variability in surface photosynthetic efficiency. The effect of nutrient limitation was clear when, in January 2004, the MLD became deeper than the top of the nutricline (Figs. 3, 4). Even though an increase in major nutrients was not detected in surface waters (Fig. 3), increased $F_V : F_M$ and decreased σ_{PSII} were characteristic

Table 4. Statistical parameters for multiple linear regressions between FRRF parameters and selected pigment concentrations at Sta. ALOHA from August 2002 to December 2004.

	Surface	DCML
	$F_V : F_M$	$F_V : F_M$
β_0	0.60	0.50
β_1 (log Chl *a*)	−0.07	−0.03
β_1 (log Chl *b*)	−0.01	0.02
β_2 (log 19′-Hex)	0.04	−0.05
β_3 (Zea)	−0.01	−0.01
β_4 (Fuco)	−0.01	0.01
r^2	0.20	0.60
p	NS	<0.05

of nutrient stress reduction (Kolber and Falkowski 1993; Suggett et al. 2003). These results are in agreement with previous investigations in the NPSG (Vaillancourt et al. 2003), which showed surface $F_V : F_M$ changes in relation to the intrusion of deep nutrient-rich waters. During January 2004, nutrient concentrations remained unchanged; rapid nutrient uptake by nutrient-starved photoautotrophs may have quickly consumed the hypothesized increase in nutrient input (Letelier et al. 2000; Vaillancourt et al. 2003). These results suggest that variations in upper-water-column FRRF parameters coupled with community-structure measurements can be used as a potential proxy, not only for photoautotrophic activity, but also for perturbations by short-lived aperiodic physical perturbations.

In addition to the role that nutrient status plays in surface photosynthetic efficiency, other environmental factors may also contribute to the observed variations in photosynthetic efficiency in the lower euphotic zone. At Sta. ALOHA, it appears that changes in community structure can influence photosynthetic efficiency in the DCML, where photosynthetic efficiency suggests nutrient-replete conditions. The apparent increase in prochlorophytes, as suggested by the rise in [Chl *b*] in absolute terms, as well as relative to [Zea], was associated with a rise in $F_V : F_M$, suggesting that floristic shifts may significantly affect the photosynthetic efficiency of the DCML. Changes in pigment concentration and ratios can be attributed to photoadaptation. However, the depth position of the DCML appears to be associated with a constant isolume (a layer of constant daily integrated photon flux; Letelier et al. 1993, 2004), which implies that the observed shifts in pigment ratio in the DCML cannot have been caused by a response of the phytoplankton assemblage to changes in light intensity. The relationship between photosynthetic efficiency and pigments could also be explained by the different fluorescence yield of each group. Different pigment composition can control the energy transfer and emission within PSII, and therefore the FRRF measurements (Suggett et al. 2001). Furthermore, under nutrient-replete conditions, different species can have different $F_V : F_M$ values (Kobližek et al. 2001). This taxon-related variability must be taken into account when interpreting the observed $F_V : F_M$ variability as changes in the photosynthetic efficiency of the phytoplankton assemblage in the DCML.

The decrease in photosynthetic efficiency below 160-m depth can be related to concomitant decrease in light availability. In this region, even though the inorganic substrate is high (N + N and SRP > 800 and 150 kg L^{-1},

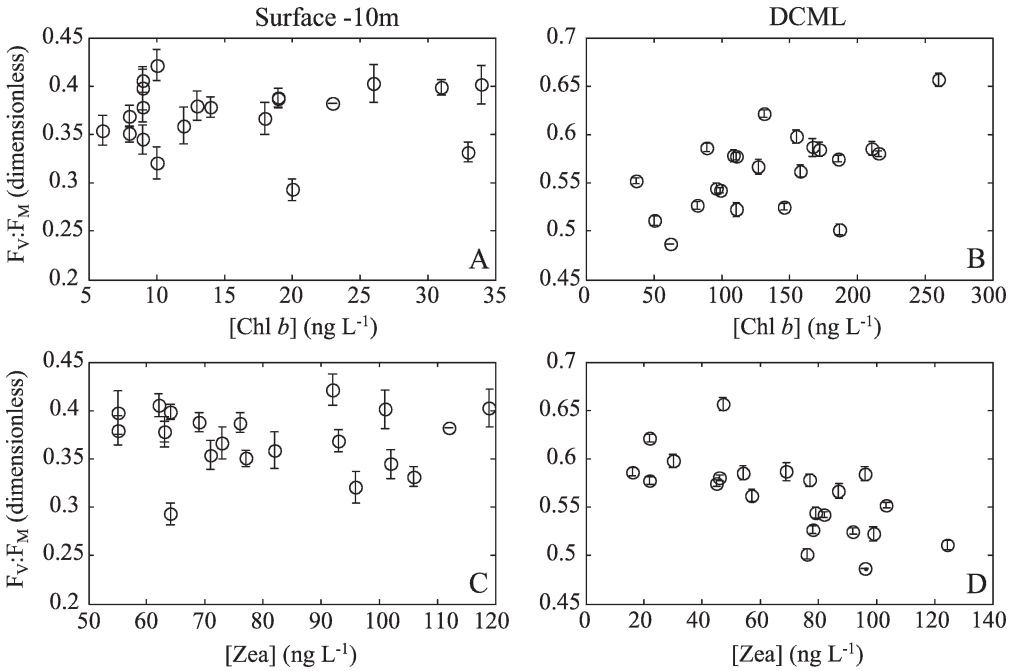


Fig. 8. Relationship among concentrations of Chl *b*, zeaxanthin, and $F_V : F_M$ for (A, C) surface and (B, D) DCML samples, respectively. Error bars represent ±1 standard error. For surface samples, all regressions were not significant. For the DCML samples, statistical parameters for the regression are given in Table 4.

Table 5. Statistical parameters for model II linear regression between photosynthetic efficiency ($F_V : F_M$) and [Chl *b*] and [Zea] in the DCML at Sta. ALOHA from August 2002 to December 2004. For each significant regression, the slope and confidence interval (CI), the *y*-intercept, and the r^2 and *p* values are given.

	$F_V : F_M$	
	[Chl *b*]	[Zea]
Slope	0.005	−0.002
y-intercept	0.43	0.61
CI slope	0.001	0.0001
r^2	0.57	0.67
P	<0.05	<0.05

respectively), light-driven photosynthesis is low due to limited photon flux. The interaction between nutrient and light in controlling photosynthetic efficiency is shown by the relationship between F_M (proxy for Chl *a* concentrations) and $F_V : F_M$ (Fig. 7). For similar low F_M values, photosynthetic efficiency varied greatly ($F_V : F_M$ range 0.25–0.60), indicating the role of high-light, low-nutrient (low $F_V : F_M$ at the surface) versus low-light, high-nutrient (low $F_V : F_M$ in the DCML) conditions in influencing photosynthetic processes.

Similar to $F_V : F_M$, σ_{PSII} is also a function of light, nutrients, temperature, species, and their relative environmental history. The rate of PSII RC closure per absorbed light, as determined by σ_{PSII}, is a measure of the "functional size" of the pigment antenna in terms of its ability to close the functional reaction centers. While a large σ_{PSII} value means large antenna relative to a small number of PSII RC (such as under nutrient depletion), a small σ_{PSII} value corresponds to a small antenna relative to a large number of PSII RC (typical of high nutrient availability; Kolber and Falkowski 1993). At the surface, high σ_{PSII} values confirmed a nutrient stress condition, as previously indicated by $F_V : F_M$ values (Fig. 2; Table 2). High σ_{PSII} values are consistent with previous patterns in nutrient-poor waters of the Pacific Ocean (Behrenfeld and Kolber 1999).

The lack of significant relationship between photosynthetic efficiency and SRP availability found here is in apparent contradiction with previous findings at Sta. ALOHA, which have suggested that in this ecosystem photoautotrophic activity is under P control (Karl 1999; Björkman et al. 2000). In contrast, results of the present investigation suggest that inorganic N may be controlling photosynthetic processes (Fig. 6; Table 3). In order to reconcile this apparent discrepancy, several explanations may be considered. First, SRP limitation may affect predominately photosynthetic microbes that can fix nitrogen gas (diazotrophs). Also, because these species contribute approximately 5–10% of the microbial photoautotrophic assemblage, changes in $F_V : F_M$ resulting from SRP limitation affecting diazotrophs may not be resolved when assessing the physiological state of the full phytoplankton assemblage. A second consideration is the bioavailability of P within a pool different from the one considered here (i.e., inorganic vs. organic) and the high recycling rate of particular P-rich compounds (i.e., nucleotides) that can confound any possible relationships between photosynthetic efficiency and P availability. At Sta. ALOHA, a fraction of dissolved organic P has been found to be bioavailable to the microbial community (Björkman and Karl 2003). Finally, the lack of a biophysical basis linking P and Chl *a* fluorescence may be responsible for the observed independence between P availability and photosynthetic parameters. While a good biophysical understanding between N-Fe availability and Chl *a* fluorescence exists (i.e., the role of N and Fe in Chl *a* synthesis, elemental constituents of RCII centers, and electron transport chain; Kolber and Falkowski 1993; Moore et al. 2006), intracellular P is more closely related to energy sources (adenosine triphosphate [ATP] and nicotinamide adenine dinucleotide phosphate [NADPH]) than to the biophysical processes occurring in PSII (such as the phosphorylation of antennae complexes to PSII and PSI), where most Chl *a* fluorescence is generated. Considering these arguments, the results presented here do not preclude a possible P control on photosynthetic processes.

Light availability can also influence σ_{PSII} (Kolber and Falkowski 1993), and this relationship could help explain the temporal σ_{PSII} variations. The seasonal cycle in surface σ_{PSII} was approximately the inverse of the seasonal light cycle at Sta. ALOHA. The increase in surface σ_{PSII} during winter can be interpreted as the ability of photoautotrophs to adapt to changes in their light environment (due to seasonal decrease in surface light and increased mixing). On the other hand, the light increase during summer may have induced a decrease in the functional size of the antenna, as photon densities became higher. Although it is not possible with the present data sets to confirm this interpretation, other lines of evidence are consistent with it. For example, Letelier et al. (1993) and Winn et al. (1995) described the increase of chlorophyll concentration per unit biomass and per cell, respectively, in surface waters of Sta. ALOHA during winter months in response to the seasonal decrease in photon flux. Nevertheless, we must also consider the role that seasonal changes in community structure may have in σ_{PSII} variability. The summer decrease in surface σ_{PSII} could be related to the increase in the relative contribution of cyanobacteria (Dore et al. 2008) or their N_2-fixation activity (Letelier and Karl 1996; Karl et al. 1997) by contributing new N to surface populations.

An updated view of the oligotrophic two-layer model—The vertical gradient in photosynthetic efficiency at Sta. ALOHA is consistent with the two-layer model proposed for this oligotrophic region (Coale and Bruland 1987; Small et al. 1987). The distinction between (1) high recycling and low new production in the upper water column and (2) low recycling and high new production in the lower euphotic zone can be extended to photosynthetic efficiency. As the present results indicate, photosynthetic processes at Sta. ALOHA are more efficient in the lower euphotic zone. The transition in photosynthetic parameters around the MLD (Figs. 2, 5) is a further indication of the physiological distinction between the upper and lower layer. This transition may be triggered by (1) particle accumulation

at this dense surface (false benthos model) and enhanced recycling and substrate availability, (2) increased diffusive flux below the MLD, and/or (3) a change in species composition.

The two-layer model for this oligotrophic region should also be considered in terms of photosynthetic temporal variability. At Sta. ALOHA, the higher temporal variability observed in photosynthetic processes at the surface relative to deep layers indicates a vertical difference in physiological and ecological stability (i.e., balance in photosynthetic processes, light absorption, transfer, and utilization). In the DCML, the low variability in photosynthetic efficiency suggests that the energy transfer (i.e., electron flow) between photosystems is well coupled and exhibits relatively little loss of energy in the forms of heat and fluorescence. It could also be interpreted such that the light energy absorbed is efficiently utilized, implying a concomitantly high yield in intracellular energy in the forms of ATP and NADPH derived from the light reactions of photosynthesis. Conversely, the high variability in the upper water column suggests an imbalance between the capture and utilization of light within PSII RC.

The vertical gradient in photosynthetic efficiency could also be related to vertical difference in photoautotroph community structure in the NPSG (Venrick 1988). The vertical distribution of key photoautotroph species indicates that a significant distinction between shallow and deep flora occurs in this environment (Venrick 1988). As different species have different fluorescence yields (and therefore different $F_V : F_M$ and σ_{PSII}), the observed vertical gradient in photosynthetic efficiency may be due, in part, to a shift in the specific composition with depth. In this context, at Sta. ALOHA, the FRRF signal is mainly dominated by *Prochlorococcus* spp. fluorescence (Campbell et al. 1994), even though the Chl *a* fluorescence yield in these species is lower than for other eukaryotic cells (Moore et al. 1995; Ting et al. 2001). The vertical transition between physiologically distinct surface and deep *Prochlorococcus* spp. populations (Moore et al. 1995) could account for a fraction of the observed variability in FRRF parameters. Furthermore, the relative increase of picoeukaryotes in the lower euphotic zone at Sta. ALOHA (Campbell et al. 1994) might also contribute to the observed vertical gradient in $F_V : F_M$, as eukaryotes tend to have higher $F_V : F_M$ values under nutrient-replete conditions than prokaryotes (Suggett et al. 2003).

Ecological implications—The vertical gradient in photosynthetic efficiency has important implications for trophic dynamics and biogeochemical cycling for this particular ecosystem. Low photosynthetic efficiency suggests that chronic nutrient limitation significantly restricts the photosynthetic activity of the surface photoautotrophic assemblage through time. This effect would be most likely found in the molecular composition of RC (N requirements for PSII RC) and of electron transport carriers (Fe requirements), since at Sta. ALOHA, the majority of Fe in the MLD is considered to be in colloidal form and, therefore, not readily available to photoautotrophs (Wu et al. 2001). This inefficiency can influence the flux of energy to higher trophic levels in surface waters. Conversely, the high photosynthetic efficiency observed in the DCML suggests high growth rates. These results are in agreement with independent growth rate estimates of *Prochlorococcus* spp. and other phototrophic eukaryotes for this environment (Laws et al. 1984; Liu et al. 1997). Since the photoautotrophic standing stock in this layer remains relatively constant, the high photosynthetic efficiency implies rapid turnover of carbon (and associated bioelements) and the importance of a removal process (both grazing and sinking).

The relationship between photosynthetic processes and environmental forcing highlights the important role of physical perturbations and community structure in influencing photosynthetic processes at Sta. ALOHA. The relatively rapid photosynthetic response following a perturbation (MLD becoming deeper than the top of the nutricline) in the upper water column confirms that surface layers are dynamic systems with fast physiological responses. Such rapid changes in photoautotrophic activity could have important consequences for biological processes, such as bloom formation (by decoupling respiration and photosynthesis) and bacteria–photoautotroph interactions. As suggested by Karl et al. (2003), sudden variations in photoautotrophic activity can control the metabolic balance of this ecosystem, and this would have implications for CO_2 atmosphere–ocean fluxes. In addition, the relationship between community structure and photosynthetic efficiency in the DCML highlights the importance of succession in ecosystems dynamics. Environmental pressure, which controls the abundance of prochlorophytes versus cyanobacteria, may result in a significant change in photoautotroph community activity, which has implications for system efficiency.

To further understand the role of environmental pressure on photosynthetic and ecological processes in this oligotrophic region, future FRRF studies should be focused on understanding the possible relationship between the availability of different P forms (inorganic vs. organic) and fluorescence transients. Such an endeavor will help to determine the role of P in influencing photosynthetic efficiency and photoautotrophic activity. The role of different photoautotrophic groups in controlling FRRF variations should also be investigated in order to understand the role of community shifts in photoautotrophic productivity of this ecosystem.

References

Behrenfeld, M. J., and Z. S. Kolber. 1999. Widespread iron limitation of phytoplankton in the South Pacific Ocean. Science **283:** 840–843.

Berger, W. H. 1989. Global maps of ocean productivity, p. 429–455. *In* W. H. Berger, V. S. Smetacek and G. Wefer [eds.], Productivity of the ocean: Present and past. Wiley.

Björkman, K. M., and D. M. Karl. 2003. Bioavailability of dissolved organic phosphorus in the euphotic zone at Station ALOHA, North Pacific Subtropical Gyre. Limnol. Oceanogr. **48:** 1049–1057.

———, A. L. Thomson-Bulldis, and D. M. Karl. 2000. Phosphorus dynamics in the North Pacific Subtropical Gyre. Aquatic Microb. Ecol. **22:** 185–198.

Campbell, L., H. A. Nolla, and D. Vaulot. 1994. The importance of *Prochlorococcus* to community structure in the central North Pacific Ocean. Limnol. Oceanogr. **39:** 954–961.

Coale, K. H., and K. W. Bruland. 1987. Oceanic stratified euphotic zone as elucidated by ^{234}Th:^{238}U disequilibria. Limnol. Oceanogr. **32:** 189–200.

Corno, G., R. M. Letelier, M. R. Abbott, and D. M. Karl. 2006. Assessing the temporal variability of primary production in the North Pacific Subtropical Gyre: A comparison of fast repetition rate fluorometry and ^{14}C measurements. J. Phycol. **42:** 51–60.

Cullen, J. J., and R. E. Davis. 2003. The blank can make a big difference in oceanographic measurements. Limnol. Oceanogr. Bull. **12:** 29–35.

Ditullio, G. R., and E. A. Laws. 1991. Impact of an atmospheric–oceanic disturbance on phytoplankton community dynamics in the North Pacific Central Gyre. Deep-Sea Res. I **38:** 1305–1329.

Dore, J. E., and D. M. Karl. 1996. Nitrite distributions and dynamics at Station ALOHA. Deep-Sea Res. II **43:** 385–402.

———, R. M. Letelier, M. J. Church, R. Lukas, and D. M. Karl. 2008. Summer phytoplankton blooms in the oligotrophic North Pacific Subtropical Gyre: Historical perspective and recent observations. Prog. Oceanogr. **76:** 2–38. doi:10.1016/j.pocean.2007.10.002.

Falkowski, P. G., R. T. Barber, and V. Smetacek. 1998. Biogeochemical controls and feedbacks on ocean primary production. Science **281:** 200–206.

Garside, C. 1982. A chemiluminescent technique for the determination of nanomolar concentrations of nitrate and nitrite in seawater. Mar. Chem. **11:** 159–167.

Grande, K., P. J. LeB. Williams, J. Marra, R. Eppley, and M. Bender. 1989. Primary production in the North Pacific Gyre: A comparison of rates determined by the ^{14}C, CO_2, and ^{18}O methods. Deep-Sea Res. I **36:** 1621–1634.

Juranek, L. W., and P. D. Quay. 2005. In vitro and in situ gross primary and net community production in the North Pacific Subtropical Gyre using labeled and natural abundance isotopes of dissolved O_2. Glob. Biogeochem. Cy. **19:** 2384–2399.

Kaiser, J., M. K. Reuer, B. Barnett, and M. L. Bender. 2005. Marine productivity estimates from continuous O_2/Ar ratio measurements by membrane inlet mass spectrometry. Geophys. Res. Lett. **32:** L19605. doi: 10.1029/2005GL023459.

Karl, D. M. 1999. A sea of change: Biogeochemical variability in the North Pacific Subtropical Gyre. Ecosystems **2:** 181–214.

———, R. R. Bidigare, and R. M. Letelier. 2001. Long-term changes in plankton community structure and productivity in the North Pacific Subtropical Gyre: The domain shift hypothesis. Deep-Sea Res. II **43:** 539–568.

———, J. R. Christian, J. E. Dore, D. V. Hebel, R. M. Letelier, L. M. Tupas, and C. D. Winn. 1996. Seasonal and interannual variability in primary production and particle flux at station ALOHA. Deep-Sea Res. II **43:** 539–568.

———, D. V. Hebel, K. Björkman, and R. M. Letelier. 1998. The role of dissolved organic matter release in the productivity of the oligotrophic North Pacific Ocean. Limnol. Oceanogr. **43:** 1270–1286.

———, E. A. Laws, P. Morris, P. J. LeB. Williams, and S. Emerson. 2003. Metabolic balance of the open sea. Nature **426:** 32.

———, R. M. Letelier, D. V. Hebel, D. F. Bird, and C. D. Winn. 1992. *Trichodesmium* blooms and new nitrogen in the North Pacific Gyre, p. 219–237. *In* E. J. Carpenter, D. G. Capone and J. G. Rueter [eds.], Marine pelagic cyanobacteria: *Trichodesmium* and other diazotrophs. Kluwer.

———, ———, L. Tupas, J. R. Dore, J. Christian, and D. Hebel. 1997. The role of nitrogen fixation in biogeochemical cycling in the subtropical North Pacific Ocean. Nature **388:** 533–538.

———, and G. Tien. 1992. MAGIC: A sensitive and precise method for measuring dissolved phosphorus in aquatic environments. Limnol. Oceanogr. **37:** 105–116.

Koblížek, M., D. Kaftan, and L. Nedbal. 2001. On the relationship between the non-photochemical quenching of the chlorophyll fluorescence and the photosystem II light harvesting efficiency. A repetitive flash fluorescence induction study. Photosynth. Res. **68:** 141–156.

Kolber, Z. S., and P. G. Falkowski. 1993. Use of active fluorescence to estimate phytoplankton photosynthesis in situ. Limnol. Oceanogr. **38:** 1646–1665.

———, O. Prasil, and P. G. Falkowski. 1998. Measurements of variable chlorophyll fluorescence using fast repetition rate techniques: Defining methodology and experimental protocols. Biochim. Biophys. Acta **1367:** 88–106.

Laney, S. R. 2003. Assessing the error in photosynthesis properties determined by fast repetition rate fluorometry. Limnol. Oceanogr. **48:** 2234–2242.

Laws, E. A., D. G. Redalje, L. W. Haas, P. K. Bienfang, R. W. Eppley, W. G. Harrison, D. M. Karl, and J. Marra. 1984. High phytoplankton growth and production rates in oligotrophic Hawaiian coastal waters. Limnol. Oceanogr. **29:** 1161–1169.

Letelier, R. M., R. R. Bidigare, D. V. Hebel, M. Ondrusek, C. D. Winn, and D. M. Karl. 1993. Temporal variability of phytoplankton community structure based on pigment analysis. Limnol. Oceanogr. **38:** 1420–1437.

———, J. E. Dore, C. D. Winn, and D. M. Karl. 1996. Seasonal and interannual variations in autotrophic carbon assimilation at Station ALOHA. Deep-Sea Res. II **43:** 467–490.

———, and D. M. Karl. 1996. The role of *Trichodesmium* spp. in the productivity of the subtropical North Pacific Ocean. Mar. Ecol. Prog. Ser. **133:** 263–273.

———, ———, M. R. Abbott, and R. R. Bidigare. 2004. Light driven seasonal patterns of chlorophyll and nitrate in the lower euphotic zone of the North Pacific Subtropical Gyre. Limnol. Oceanogr. **49:** 508–519.

———, ———, ———, P. Flament, M. Freilich, R. Lukas, and T. Strub. 2000. Role of late winter mesoscale events in the biogeochemical variability of the upper water column of the North Pacific Subtropical Gyre. J. Geophys. Res. **105:** 28723–28740.

Levitus, S. 1982. Climatological atlas of the world ocean. NOAA Professional Paper 13. U.S. Govt. Print Office.

Liu, H., H. A. Nolla, and L. Campbell. 1997. *Prochlorococcus* growth rate and contribution to primary production in the equatorial and subtropical North Pacific Ocean. Aquat. Microb. Ecol. **12:** 39–47.

Mackey, M. D., D. J. Mackey, H. W. Higgins, and S. W. Wright. 1996. CHEMTAX—a program for estimating class abundances from chemical markers: Application to HPLC measurements of phytoplankton. Mar. Ecol. Prog. Ser. **144:** 265–283.

McArdle, B. H. 2003. Lines, models, and errors: Regression in the field. Limnol. Oceanogr. **48:** 1363–1366.

Moore, C. M., M. M. Mills, A. Milne, R. Langlois, E. P. Achterberg, K. Lochte, J. La Roche, and R. J. Geider. 2006. Iron limits primary productivity during spring bloom development in the central North Atlantic. Glob. Change Biol. **12:** 626–634.

Moore, L. R., R. Goericke, and S. W. Chisholm. 1995. Comparative physiology of *Synechococcus* and *Prochlorococcus*: Influence of light and temperature on growth, pigments, fluorescence and absorptive properties. Mar. Ecol. Prog. Ser. **116:** 259–275.

Ondrusek, M. E., R. R. Bidigare, K. Waters, and D. M. Karl. 2001. A predictive model for estimating rates of primary production in the subtropical North Pacific Ocean. Deep-Sea Res. II **48:** 1837–1863.

Peterson, B. J. 1980. Aquatic primary productivity and ^{14}C-CO_2 method: A history of the productivity problem. Ann. Rev. Ecol. Syst. **11:** 359–385.

Platt, T. 1984. Primary productivity in the central North Pacific: Comparison of oxygen and carbon fluxes. Deep-Sea Res. I **31:** 1311–1319.

Sakamoto, C. M., D. M. Karl, H. W. Jannasch, R. R. Bidigare, R. M. Letelier, P. M. Walz, J. P. Ryan, P. S. Polito, and K. S. Johnson. 2004. Influence of Rossby waves on nutrient dynamics and the plankton community structure in the North Pacific Subtropical Gyre. J. Geophys. Res. **109:** 1976–1988.

Small, L. F., G. A. Knauer, and M. D. Tuel. 1987. The role of sinking fecal pellets in stratified euphotic zone. Deep-Sea Res. I **34:** 1705–1712.

Steeman-Nielsen, E. 1951. Measurement of the production of organic matter in the sea by means of carbon-14. Nature **167:** 684–685.

Suggett, D. J., P. Kraay, P. Holligan, M. Davey, J. Aiken, and R. Geider. 2001. Assessment of photosynthesis in a spring cyanobacterial bloom by use of a fast repetition rate fluorometer. Limnol. Oceanogr. **46:** 802–810.

———, K. Oxborough, N. R. Baker, H. L. Macintyre, T. M. Kana, and R. J. Geider. 2003. Fast repetition rate and pulse amplitude modulation chlorophyll *a* fluorescence measurements for assessment of photosynthetic electron transport in marine phytoplankton. Eur. J. Phycol. **38:** 371–384.

Ting, C. S., G. Rocap, J. King, and S. W. Chisholm. 2001. Phycobiliprotein genes of the marine photosynthetic prokaryote *Prochlorococcus*: Evidence for rapid evolution of genetic heterogeneity. Microbiol. **147:** 3171–3182.

Vaillancourt, R. D., J. Marra, M. P. Seki, M. L. Parsons, and R. R. Bidigare. 2003. Impact of a cyclonic eddy on phytoplankton community structure and photosynthetic competency in the subtropical North Pacific Ocean. Deep-Sea Res. I **50:** 829–847.

Venrick, E. L. 1988. The vertical distributions of chlorophyll and phytoplankton species in the North Pacific central environment. J. Plankton Res. **10:** 987–998.

Williams, P. J. LeB., P. J. Morris, and D. M. Karl. 2004. Net community production and metabolic balance at the oligotrophic ocean site, station ALOHA. Deep-Sea Res. I **51:** 1563–1578.

Winn, C. D., L. Campbell, J. Christian, R. M. Letelier, D. V. Hebel, J. E. Dore, L. Fujieki, and D. M. Karl. 1995. Seasonal variability in the phytoplankton community of the North Pacific Subtropical Gyre. Glob. Biogeochem. Cy. **9:** 605–620.

Wu, J., E. Boyle, W. Sunda, and L. Wen. 2001. Soluble and colloidal iron in the oligotrophic North Atlantic and North Pacific. Science **293:** 847–849.

Received: 19 June 2006
Accepted: 19 June 2007
Amended: 6 February 2008